Published in final edited form as:
Cancer Res. 2007 May 1; 67(9): 4104–4112. doi:10.1158/0008-5472.CAN-06-4672.

Identification of Novel Amplification Gene Targets in Mouse and Human Breast Cancer at a Syntenic Cluster Mapping to Mouse Identification of Novel Amplification Gene Targets in Mouse and Human Breast Cancer at a Syntenic Cluster Mapping to Mouse ch8A1 and Human ch13q34

Martin C. Abba[1], **Victoria T. Fabris**[1], **Yuhui Hu**[1], **Frances S. Kittrell**[2], **Wei-Wen Cai**[2], **Lawrence A. Donehower**[2], **Aysegul Sahin**[3], **Daniel Medina**[2], and **C. Marcelo Aldaz**[1]

[1]Department of Carcinogenesis, The University of Texas M. D. Anderson Cancer Center, Science Park-Research Division, Smithville, Texas

[2]Baylor College of Medicine

[3]Department of Pathology, The University of Texas M. D. Anderson Cancer Center, Houston, Texas

Abstract

Serial analysis of gene expression from aggressive mammary tumors derived from transplantable p53 null mouse mammary outgrowth lines revealed significant up-regulation of *Tfdp1* (*transcription factor Dp1*), *Lamp1* (*lysosomal membrane glycoprotein 1*) and *Gas6* (*growth arrest specific 6*) transcripts. All of these genes belong to the same linkage cluster, mapping to mouse chromosome band 8A1. BAC-array comparative genomic hybridization and fluorescence *in situ* hybridization analyses revealed genomic amplification at mouse region ch8A1.1. The minimal region of amplification contained genes *Cul4a*, *Lamp1*, *Tfdp1*, and *Gas6*, highly overexpressed in the p53 null mammary outgrowth lines at preneoplastic stages, and in all its derived tumors. The same amplification was also observed in spontaneous p53 null mammary tumors. Interestingly, this region is homologous to human chromosome 13q34, and some of the same genes were previously observed amplified in human carcinomas. Thus, we further investigated the occurrence and frequency of gene amplification affecting genes mapping to ch13q34 in human breast cancer. *TFDP1* showed the highest frequency of amplification affecting 31% of 74 breast carcinomas analyzed. Statistically significant positive correlation was observed for the amplification of *CUL4A*, *LAMP1*, *TFDP1*, and *GAS6* genes ($P < 0.001$). Meta-analysis of publicly available gene expression data sets showed a strong association between the high expression of *TFDP1* and decreased overall survival ($P = 0.00004$), relapse-free survival ($P = 0.0119$), and metastasis-free interval ($P = 0.0064$). In conclusion, our findings suggest that *CUL4A*, *LAMP1*, *TFDP1*, and

Requests for reprints: C. Marcelo Aldaz, Department of Carcinogenesis, The University of Texas M. D. Anderson Cancer Center, Science Park-Research Division, P.O. Box 389, Smithville TX 78957. Phone: 512-237-2403; Fax: 512-237-2475; maaldaz@mdanderson.org.

Note: M.C. Abba, V.T. Fabris, and Yuhui Hu contributed equally to this work.

Competing interests statement: The authors declare that they have no competing financial interests.

GAS6 are targets for overexpression and amplification in breast cancers. Therefore, overexpression of these genes and, in particular, *TFDP1* might be of relevance in the development and/or progression in a significant subset of human breast carcinomas.

Introduction

Genetically engineered mouse models of mammary cancer have been developed as tools to study molecular pathways involved in human breast carcinogenesis. The p53 null model of mammary carcinogenesis reproduces many of the critical features of human breast cancer (1, 2). In this model, BALB/c p53 null mammary epithelial cells are transplanted into cleared mammary fat pads of p53 wild-type syngeneic hosts. More than 60% of these isogenic orthotopic transplants develop invasive mammary adenocarcinomas and, upon hormonal stimulation 100% of the grafts, are tumorigenic (1). Most of these tumors are intraductal in origin, and premalignant lesions can be observed, closely mimicking human breast cancer. Medina et al. derived serially transplantable ductal premalignant mammary outgrowth lines from p53 null mammary epithelium. These premalignant outgrowth lines are mostly aneuploid and estrogen/progesterone receptor positive. They are characterized by the in vivo development of ductal hyperplasias that systematically progress to invasive mammary tumors (3).

Two general patterns of stable growth were mostly observed. One predominantly ductal, composed of small ducts, few lobules, and infrequent alveoli. This mildly aggressive phenotype is represented by a mammary outgrowth line named PN1B. At various times after transplantation, a progressive epithelial dysplasia and hyperplasia of various degrees of aggressiveness could be observed. This line produced only 15% of tumors at 12 months after transplantation. The second pattern observed is represented by the much more aggressive mammary outgrowth line named PN1A, with predominantly ductal outgrowth by 8 weeks post-transplantation; by 14–16 weeks, the ducts were organized as small lobules, and the lumen of all alveolar units were filled by cells. The PN1A line is spontaneously highly tumorigenic with a short latency period, 78% mammary adenocarcinomas developed within 6 months after transplantation in the host mammary fat pad (3).

Recently, we reported the results of human-mouse comparative global gene expression studies on mammary tumors using the p53 null model and human breast carcinomas (4). In the course of these studies, we noticed that some of the mouse p53 null tumors analyzed showed dramatic overexpression of a cluster of genes located close to the centromere of mouse chromosome 8 band A1, indicative of a potential gene amplification phenomenon. In particular, this was first observed from a p53 null mammary tumor derived from the above-described PN1A premalignant outgrowth line.

The primary goal of this study was to better characterize the chromosomal basis and frequency for the observed overexpression of genes mapping to mouse ch8A1.1. We present data supporting the occurrence of genomic amplification affecting the ch8A1.1 region in mouse mammary tumors. Furthermore, we show that amplification of the homologous syntenic cluster mapping to human ch 13q34 also affects subsets of human breast cancers. This interspecies similarity suggests that amplification of gene targets mapping to this

homologous genomic region, both in human and mouse, might be of much significance in breast carcinogenesis.

Materials and Methods

Serial analysis of gene expression of mouse mammary samples

Serial analysis of gene expression (SAGE) libraries from p53 null mammary tumors was done as previously described (5). Additional p53 null mammary tumors were dissected and snapped frozen for RNA isolation and validation studies. As normal control for SAGE and Northern analyses, enriched normal mammary epithelium from p53 null transplants was used (5). We employed the mSAGE Digital Expression Displayer algorithm available at the Cancer Genome Anatomy Project[4] to identify statistically significant different expressed genes between SAGE libraries ($P \leq 0.01$).

Northern blot analyses

We did Northern analysis of the genes Ing1 (inhibitor of growth family 1), Cul4a (Cullin 4a), Lamp1 (lysosomal membrane glycoprotein 1), Tfdp1 (transcription factor Dp1), and Gas6 (growth arrest specific 6) in the two premalignant p53 null mammary outgrowth lines PN1A and PN1B in various mammary tumors derived from the PN1A line and in various spontaneously generated p53 null tumors not derived from the outgrowth lines. Total RNA was isolated from mouse samples, gene probes generated, and hybridization done as previously described using standard procedures (6).

Whole-genome mouse bacterial artificial chromosome microarray comparative genomic hybridization

The whole-genome bacterial artificial chromosome (BAC) array used contained 19,000 unique BAC clones from mouse genomic libraries spaced at 0.5-Mb interval. Comparative genomic hybridization was done on DNA isolated from two p53 null mouse mammary tumors. One of the tumors was derived from the PN1A outgrowth line (2860R), and the other was a spontaneously generated tumor (8813R). CGH analyses were done as previously described with minor modifications (7).

Fluorescence *in situ* hybridization analysis

Chromosomal amplification of mouse chromosome 8A1 region was further studied by interphase and cytogenetics fluorescence *in situ* hybridization (FISH). We did FISH analyses with eight BACs (RP23-434M17, RP23-270K21, RP23-368G24, RP23-478E13, RP23-167K11, RP23-133J23, RP23-470N10, and RP23-172L10). BACs were labeled by random priming using biotin-16-dUTP and hybridized to interphase nuclei or metaphase chromosomes. Fluorescent signals were detected with FITC-avidin, and the nuclei were counterstained with 4′,6-diamidino-2-phenylindole (DAPI).

[4] http://cgap.ncb.nih.gov/SAGE/

Real-time quantitative PCR analyses on DNA from human breast carcinomas

Snapped frozen human breast carcinoma samples were obtained from the M.D. Anderson Breast Cancer Tumor Bank. DNA from 74 human invasive breast carcinomas was extracted using the DNAeasy Tissue Kit (Qiagen Sciences). DNA duplex real-time PCR was done using the TaqMan Fast Universal PCR Master Mix (Applied Biosystems) and the 7900 HT Fast Real-Time PCR System (Applied Biosystems). The $\Delta\Delta C_T$ method was applied, and the ΔC_T value of a human normal skin fibroblast cell strain (SK50, from the American Type Culture Collection, cells not immortal) run in parallel with each assay was used for normalization to get the relative quantification for each tumor or cell line sample versus a normal chr13 gene copy number control (SK50). In the duplex PCR reactions, *paraspeckle protein 1* (*PSPC1*), located at 13q12.11, was used as the internal reference control gene. Four genes located at 13q34, *CUL4A*, *LAMP1*, *TFDP1*, and *GAS6*, were assessed. The primers and probes for each of the genes tested are *TFDP1* (forward primer, 5′-cgcaacaggaaaggagagaaga-3′; reverse primer, 5′-accttctcgcagaccttcatg-3′; and probe, FAM-agaaatgccgtaggcccttgcca-TAMRA); *CUL4A* (forward primer, 5′-agggctcgac-cacttactggat-3′; reverse primer, 5′-cctcacccggctgaacag-3′; and probe, FAM-agaacagagtgccggacctcgca-TAMRA); *GAS6* (forward primer, 5′-gagcgaggactg-[4] tatcatctgaac-3′ reverse primer, 5′-caggctgcacgaggtcctt-3′; and probe, FAM-tgaccgtgggaggtattcccttccat-TAMRA); and *LAMP1* (forward primer, 5′-gccacagtcggcaattccta-3′; reverse primer, 5′-ctgaaaacgccttcgtgaca-3′; and probe, FAM-cgtgctcctccgcgttgcactt-TAMRA); for the control gene *PSPC1*, forward primer is 5′-caactatacctggcccaccaat-3′, reverse primer is 5′-actgctccattatctggcatca-3′, and probe is VIC-atatttgcggctccttctggtcccatg-TAMRA After amplification, the obtained real-time PCR values of each tested gene is compared relative to the amplification of the internal control gene (from each duplex reaction) and represented as ΔC_T, whereas the $\Delta\Delta C_T$ $\Delta\Delta C_T$ value represents the value of each tested sample normalized in turn to amplification on DNA from the normal human skin fibroblast cell strain (SK50). Samples were considered to be affected by genomic amplification for each of the genes assayed when the $\Delta\Delta C_T$ was greater than +3 SD [99% confidence interval (99% CI); $P < 0.001$] with respect to the values observed for the SK50 (ΔC_T) reference normal control sample. All samples were analyzed in triplicate to confirm the obtained values.

Additional statistical analyses

Multivariate analysis was done by principal component analysis (PCA). Variables were codified and transformed as follows: negative staining (0) and positive staining (1) for ER/PR, Ki67 expression; lymph node negative (0) and lymph node positive (1) status; low (1), moderate (2), and high (3) tumor grade, nonrecurrent (0) and recurrent (1) tumors. To enable visualization of the factorial analysis, we employed a three-dimensional representation of the component plot in rotated space. The basic significance level was fixed at $P < 0.05$, and all data were analyzed using SPSS statistical software (SPSS Inc.).

Explorative gene expression profiling and clinical data analysis

To further investigate correlations and frequency of transcriptional up-modulation of *CUL4A*, *LAMP1*, *TFDP1*, and *GAS6* gene expression profiles and clinicopathologic parameters on larger breast carcinoma sets, data were obtained from publicly available

breast cancer microarray sets (8–13). The Oncomine cancer microarray database (14) and the Integrated Tumor Transcriptome Array and Clinical Data Analysis (ITTACA; ref. 15) resources were employed for data analysis. The Oncomine database is an integrated bioinformatic resource providing data collection, processing, and storage of all publicly available cancer microarray studies. All data are log transformed, median centered per array, and SD normalized to one per array. The gene module application lists all differential expression analyses in which the target genes were included, and allows the user to select studies of interest providing comparative statistical analyses. The Oncomine gene module application was employed for differential expression analysis (two-sided *t* test). We used a meta-analysis approach to determine the overall summary of expression patterns on genes of interest from seven independent studies. We computed summary estimates (effect size) of gene expression changes by the standardized mean difference method using the exact *t* values and sample size for each groups. To calculate the pooled effects of the selected gene profiles, each study was weighted by the inverse of the individual and between-study variance according to a random-effects model. Meta-analysis was carried out using Comprehensive Meta-analysis software (Biostat, Inc.). All effect sizes were presented with 95% CI based on the estimated variances. Kaplan-Meier analysis was assessed using the Van de Vijver et al. (10) data by means of ITTACA web interface. Two patient's groups were generated based on the median expression value of the overall distribution for each gene analyzed (e.g., TFDP1 median, −0.022; high expression, greater than −0.022; and low expression, less than −0.022).

Results

Serial analysis of gene expression

Inspection of the most highly differentially expressed transcripts between p53 null mammary tumor (TG7) versus enriched normal mammary epithelium from p53 null transplants showed that the TG7 tumor displayed dramatic overexpression of *Tfdp1* (P = 0.0001), *Lamp1* (P = 0.0001), *Gas6* (P = 0.0001), and *Ing1* (P = 0.0001; Table 1). These transcripts all belong to the same linkage cluster, located at mouse chromosome 8 band A1.1. The TG7 p53 null mammary tumor was derived from a highly tumorigenic mammary outgrowth line (PN1A; ref. 3). Furthermore, SAGE results were independently confirmed by using Affymetrix oligonucleotide microarrays, where *Ing1* (fold change, 3), *Cul4a* (gene also mapping to the same linkage group; fold change, 5), *Lamp1* (fold change, 6), *Tfdp1* (fold change, 8.5), and *Gas6* (fold change, 11) were detected overexpressed in the PN1A premalignant mammary outgrowth line. Thus, overexpression of the aforementioned genes was already observed at premalignant stages of the mammary outgrowth line PN1A before the generation of tumors.

Northern blot analysis

To validate the described findings, we did Northern analysis of the genes *Ing1*, *Lamp1*, *Tfdp1*, *Cul4a*, and *Gas6* in two premalignant p53 null mammary outgrowth lines, PN1A (highly tumorigenic) and PN1B (mildly tumorigenic; ref. 3), in various mammary tumors derived from the PN1A line and in p53 null normal mammary epithelium (Fig. 1A). *Cul4a*, *Lamp1*, and *Tfdp1* were overexpressed in the more aggressive line (PN1A) and all its

derived tumors, whereas *Ing1* and *Gas6* were increased in the PN1A line and in some of the tumors. None of the five genes were significantly overexpressed in the less aggressive PN1B outgrowth line or in normal mammary epithelium (Fig. 1A).

We also tested whether this observation extended beyond the PN1A line and its derived tumors; thus, we did Northern blot analysis of genes *Cul4a*, *Tfdp1*, and *Lamp1* in spontaneously generated p53 null mammary tumors (i.e., not derived from outgrowth lines; Fig. 1B). We observed that indeed, the three genes were overexpressed in 9 out of 10 tumors when compared with normal mammary epithelium and highly overexpressed in some tumors (e.g., T4033, Fig. 1B).

BAC array CGH analysis

To determine whether genomic amplification was the reason for overexpression of the aforementioned genes, we used CGH on high-density mouse BAC arrays. BAC-CGH was done on DNA isolated from two p53 null mouse mammary tumors. One of the tumors was derived from the p53 null PN1A mammary outgrowth line (2860R, see Fig. 1A, *first tumor on right*), and the other was a spontaneously generated p53 null tumor (8813R).

Notably, the single consistent genomic change affecting both tumors throughout the genome was that affecting mouse chromosome 8. A minor peak of potential overrepresentation was also observed affecting chromosome 15 but only in one of the tumors (2860R), followed by an apparent copy number loss affecting the proximal portion of chromosome 7 in both tumors (Fig. 2A).

Chromosome 8 presented a region of BAC clones, hybridizing with very high intensity ratios, indicative of a gene amplification phenomenon (Fig. 2A). This region of chromosomal gain was located close to the centromere of chromosome 8 band A1.1. The amplified sequences affecting both tumors were located between 3 and 14 Mb from the centromere. Two subregions of amplification could be identified; one located at 3 to 3.4 Mb and the other at 12 to 14 Mb. This confirmed the gene expression studies. The amplified genes at the 12- to 14-Mb region included *Cul4a*, *Lamp1*, *Tfdp1*, and *Gas6*, all within the same amplicon (Fig. 2B).

FISH analysis

The amplified region, relatively close to the centromeric portion of mouse chromosome 8, was also studied by means of interphase FISH. We used selected BAC clones as probes based on the BAC-CGH results (Fig. 3A). We did FISH on touch imprint preparations of p53 null mammary tumors. A high level of amplification was observed for BAC clones, RP23-478E13 (*Lamp1* gene), and RP23-167K11 (*Tfdp1* gene). Clones RP23-133J23 (*Gas6* gene) and RP23-434M17 (closer to the centromere) displayed moderate amplification, whereas clones RP23-470N10 and RP23-270K21 were not amplified in this tumor, thus defining boundaries to the amplicon (Fig. 3B). Clone RP23-172L10, located at chromosome band 8C1, was used as control of a region without amplification (data not shown).

We also did FISH analyses on metaphases obtained from the PN1A outgrowth line growing *in vitro*. The PN1A cell line presented a hypertriploid-hypotetraploid karyotype. Metaphases

displayed three to six copies of chromosome 8. All metaphases displayed two or three marker chromosomes, a metacentric chromosome with a homogenously staining region (HSR) in the centromeric portion of one of the arms (Fig. 3C, *M1*), and a small acrocentric chromosome with an HSR in the terminal portion of the chromosome (Fig. 3C, *M2*). A large acrocentric chromosome with a bright DAPI banding pattern (Fig. 3C, *M3*) was also observed. The sequences located at 3 to 3.4 Mb (RP23-434M17) and at 12 to 14 Mb from the centromere of mouse chromosome 8 (Fig. 3C) hybridized to the HSRs of the markers, suggesting the presence of numerous copies in tandem of both chromosomal regions. For this analysis, we included BAC clone RP23-368G24 (near the *Cul4a* gene), and as observed, it was also shown to be amplified.

Real-time quantitative PCR analysis on DNA from human breast carcinomas

The homologous region to mouse chromosome 8A maps in *Homo sapiens* to chromosome band 13q34. To investigate whether any of the target genes observed amplified in mouse mammary tumors was also amplified in human breast carcinomas, we analyzed DNA obtained from 74 primary breast cancer samples. Real-time quantitative PCR (Q-PCR) for the human homologous genes *CUL4A*, *LAMP1*, *TFDP1*, and *GAS6* was done. Interestingly, genomic amplification was detected for *CUL4A* in 25.7% (19 out of 74), *LAMP1* in 13.5% (10 out of 74), *TFDP1* in 31.1% (23 out of 74), and *GAS6* in 13.5% (10 out of 74). Simultaneous amplification of all four genes was observed in only 11% (8 out of 74) of tumors (Fig. 4A). Data in Fig. 4A is represented as a heat map of amplified human breast carcinomas based on using the quantitative DNA real-time PCR method described in Materials and Methods. Experiments were done in triplicate for each data point. Results are expressed as log 2 transformation of the mean difference between tumor versus normal control ($P < 0.01$). Red intensity is a representative of mean difference for each breast tumor (Fig. 4A). It is worth noting that these values do not represent specific copy number increases, but are directly proportional to the level of amplification. PCA identified statistically significant positive correlations between amplification of *CUL4A*, *LAMP1*, *TFDP1*, and *GAS6* genes ($P < 0.001$; Fig. 4B). The strongest correlation was detected between *TFDP1* and *CUL4A* gene amplification (τ -b = 0.920; $P < 0.0001$; Fig. 4C). It is worth noting that the amplification of genes *CUL4A* (τ -b = 0.375; $P = 0.01$) and *TFDP1* (τ -b = 0.311; $P = 0.029$) correlated with positive lymph node (N) status (Fig. 4C).

Gene expression profiling analysis in human breast carcinoma

To further explore the clinical relevance of *CUL4A*, *LAMP1*, *TFDP1*, and *GAS6* expression in human breast carcinomas, we evaluated information on publicly available breast cancer gene expression (microarrays) data sets. Clinicopathologic and gene expression data from breast carcinomas from various studies were collected and analyzed using Oncomine and ITTACA database resources (see Materials and Methods). Because the estrogen receptor (ER) plays a critical role in breast cancer, we first analyzed gene expression profiles of these genes relative to ER status and tumor grade. Oncomine analysis showed that *TFDP1* overexpression is associated with ER-negative ($P = 0.0001$) and high-grade ($P = 0.009$) breast carcinomas (Fig. 5A). Nonstatistically significant correlations were detected for *CUL4A*, *LAMP1*, and *GAS6* expression for ER and tumor grade ($P > 0.05$). Next, we analyzed *CUL4A*, *LAMP1*, *TFDP1*, and *GAS6* expression profiles with patient outcome

using the microarray data set of Van de Vijver et al. (10) by means of the ITTACA resource. Kaplan-Meier analysis revealed that *TFDP1* overexpression was significantly associated with shorter overall survival ($P = 0.00004$), relapse-free survival ($P = 0.0119$), and metastasis-free interval ($P = 0.0064$; Fig. 5B). Nonstatistically significant associations were detected for *CUL4A*, *LAMP1*, and *GAS6* transcripts ($P > 0.05$).

Discussion

DNA amplification is a common mechanism used by cancer cells to up-regulate the activity of critical genes, associated with tumor development and progression. Genes involved in amplification are usually known to be oncogenes, growth or transcription factors, coactivators of transcription, and positive regulators of the cell cycle in general. Several genes were observed amplified in human breast cancer, the most prominent being *ERBB2* (17q12), *MYC* (8q24), and *CCND1* (11q13). Usually, genomic amplification is associated with poor prognosis, e.g., *ERBB2* amplification and overexpression in breast cancers. The identification of specific genomic amplification events is of much importance because it could allow the development of targeted therapeutic approaches to specific breast cancer subsets. This is best illustrated by the success story of therapeutic approaches geared at neutralizing the effects of *ERBB2* overexpression in breast cancer (16).

We detected a dramatic co–up-regulation of *Ing1*, *Cul4a*, *Lamp1*, *Tfdp1*, and *Gas6* genes in p53 null mammary tumors, pointing to a possible gene amplification phenomenon. Whole-genome mouse BAC array CGH identified the chromosome 8 band A1.1 as a primary target of gene amplification in p53 null mammary tumors. Northern blot analyses showed that these genes were observed overexpressed in many spontaneously originating p53 null mouse mammary tumors.

Because the observed amplification of the ch8A1 region occurred in a p53 null background, the possibility exists that such phenomenon could be linked to the lack of an active p53 protein. Lack of a functional p53 protein has been associated with genomic instability and specifically with facilitating the occurrence of genomic amplification (17, 18). The amplification and over-expression of genes mapping to the mouse ch8A1 represent an early event in mammary gland malignant transformation as overexpression of these genes occurred in the premalignant outgrowth line PN1A. The overexpression of these genes could facilitate progression to an invasive phenotype because this overexpression was not detected in the weakly tumorigenic PN1B mammary outgrowth line.

Interestingly, some of the genes belonging to the homologous syntenic gene cluster mapping to human ch13q34 were reported to be amplified and overexpressed in a wide variety of carcinoma types including breast cancer. A high level of chromosomal gain was detected affecting ch13q34 by CGH in primary hepatocellular carcinoma and tumor cell lines (19). Similar observations were reported affecting esophageal squamous cell carcinoma (20). Furthermore, in both types of tumors, the target gene for amplification and overexpression was reported to be the *TFDP1* gene. The *CUL4A* and *CDC16* genes, located in the same region at ch13q34, in another report were also found amplified and overexpressed in hepatocellular carcinoma (21). Up-regulation of *TFDP1* was also detected in lung

adenocarcinoma (22). Notably, several years ago, amplification of *CUL4A* was reported in 16% of primary breast tumors, and 47% showed overexpression of *CUL4A* (23).

To determine recurrent genetics alterations affecting ch13q34, we analyzed DNA samples from a set of human breast cancers by real-time Q-PCR. *TFDP1* showed the highest frequency of amplification with 31% of cases followed by *CUL4A* gene with ˜26% of the breast carcinoma analyzed. All four genes were amplified in only 11% invasive of breast carcinomas. PCA identified statistically significant positive correlations among the amplification of *CUL4A*, *LAMP1*, *TFDP1*, and *GAS6* genes ($P < 0.001$). To further investigate the clinical significance of *CUL4A*, *LAMP1*, *TFDP1*, and *GAS6* overexpression in human breast carcinoma, we search for significant correlations on publicly available breast cancer gene expression data sets. Kaplan-Meier analysis revealed that *TFDP1* overexpression was significantly associated with shorter overall survival, relapse-free survival, and metastasis-free interval. In addition, *TFDP1* overexpression correlated with the loss of ER status and high-grade breast carcinomas (Fig. 5A). These data are in line with a number of studies showing that most ER-positive tumors are of low grade, and high-grade tumors are mainly ER negative. It has been proposed that tumor breast cancer progression is characterized by a shift from the well-differentiated (low-grade) to the poorly differentiated (high-grade) state (perhaps by loss of ER-positive status). In this sense, *Tfdp1* overexpression could play an important role in early mouse or human breast tumorigenesis, accelerating tumor progression toward more aggressive stages. Furthermore, these data showed that at least *TFDP1* overexpression behaves as a poor prognostic indicator in human breast cancer.

TFDP1 encodes the transcription factor DP1 that forms heterodimers with E2F protein family members. The transcriptional activator complex E2F/DP is known to be critical for cell cycle progression. E2F1/DP1 are implicated in cell cycle progression by regulating the genes in which products are required for DNA synthesis (DNA polymerase α, thymidine kinase); those that encode nuclear oncoproteins (C-MYC, N-MYC, and B-MYB); and those that encode cell cycle regulators (cyclin A, cyclin E, CDC2, and RB; refs. 24, 25). DP proteins are endowed with proto-oncogenic activity (26, 27). Overexpression of DP1 or DP2, together with activated HA-RAS, causes a transformation of rat embryo fibroblasts in the absence of a cotransfected *E2F* family member (26). Transgenic mouse lines expressing *DP1* under the control of a keratin-5 promoter displayed hyperplasia and hyperproliferation of the epidermis (28). Although mice did not develop spontaneous tumors, when exposed to a two-stage chemical carcinogenesis protocol, more and larger skin tumors developed in *K5/DP1* transgenic mice than in nontransgenic mice (28). Coexpression of DP1 and E2F increases proliferation and enhances carcinogenesis.

CUL4A (*Cullin 4a*) belongs to the family of cullin proteins that are essential components of a multifunctional ubiquitin-protein ligase E3 complex. Recent studies showed that CUL4A is associated with damaged DNA binding protein, which stimulates E2F1-activated transcription. In addition, it was shown that CUL4A physically associated with MDM2 and participates in the proteolysis of p53 (29). As mentioned, *CUL4A* was observed amplified in human breast cancer and hepatocellular carcinoma (19, 23). Overexpression of *CUL4A* in *MCF10A* resulted in anchorage-independent growth and the disruption of the G_2-M cell

cycle checkpoint after ionizing radiation (30). These results suggest a role for *CUL4A* in tumorigenesis and/or tumor progression, possibly through disruption of cell cycle control.

LAMP1 is a lysosomal membrane glycoprotein expressed in the cell surface. Interestingly, an increase in expression of cell surface of LAMPs was found associated with the metastatic potential of human colon cancer cell lines (31). This glycoprotein is able to bind E- and P-selectins that are expressed on vascular endothelium and could facilitate the adhesion of tumoral cells to the endothelium and promote the metastatic process (32).

GAS6 is a secreted protein with structural homology to members of a superfamily of basement membrane proteins implicated in the growth and differentiation of many cells. GAS6 was found over-expressed in human endometrial and ovarian cancer (33). GAS6 is, thus far, the single activating ligand for AXL (34). AXL is a receptor tyrosine kinase that has been reported to induce cell proliferation and transformation (35). In mice, Axl is expressed in the normal mammary gland and overexpressed in aggressive mammary tumors. Several studies suggested that the GAS6/AXL signaling regulates processes vital for both neovascularization and tumorigenesis (36). GAS6/AXL interactions that may be involved in directed cell migration has been suggested for vascular smooth muscle cells in the context of remodeling of the vessel wall after vascular injury and for endothelial cells during tumor angiogenesis (37).

Taken together, these findings suggest that the amplification and overexpression of specific gene(s) located in mouse ch8A1 or comparatively the homologous syntenic gene cluster on human ch13q34 could play an important role in early mouse or human breast carcinogenesis, respectively. The fact that the observation is common to both species highlights the relevance and potential significant implications of the identified genomic amplification. Furthermore, the striking similarity between mouse and human breast carcinogenesis on the occurrence of this particular genomic aberration validates the use of this mouse system as an excellent surrogate model for understanding the mechanistic implications and *in vivo* consequences of this phenomenon. We speculate that the key genes driving the amplification phenomenon are likely *TFDP1* and perhaps *CUL4A*. Further studies are needed to confirm this speculation and to clarify the functional significance of overexpression of each member of the identified amplicon. However, it is also possible that the coactivation of more than one target from the identified amplicon may contribute in a synergistic manner to breast cancer development and progression.

Acknowledgments

Grant support: NIH-National Cancer Institute grants U19 CA84978 (C.M. Aldaz), U01CA84243, and National Institute of Environmental Health Sciences center grant ES-07784.

References

1. Jerry DJ, Kittrell FS, Kuperwasser C, et al. A mammary-specific model demonstrates the role of the p53 tumor suppressor gene in tumor development. Oncogene. 2000; 19:1052–8. [PubMed: 10713689]
2. Medina D, Kittrell FS. p53 function is required for hormone-mediated protection of mouse mammary tumorigenesis. Cancer Res. 2003; 63:6140–3. [PubMed: 14559792]

3. Medina D, Kittrell FS, Shepard A, et al. Biological and genetic properties of the p53 null preneoplastic mammary epithelium. FASEB J. 2002; 16:881–3. [PubMed: 11967232]
4. Hu Y, Sun H, Drake J, et al. From mice to humans: identification of commonly deregulated genes in mammary cancer via comparative SAGE studies. Cancer Res. 2004; 64:7748–55. [PubMed: 15520179]
5. Aldaz CM, Hu Y, Daniel R, Gaddis S, Kittrell F, Medina D. Serial analysis of gene expression in normal p53 null mammary epithelium. Oncogene. 2002; 21:6366–76. [PubMed: 12214277]
6. Charpentier AH, Bednarek AK, Daniel RL, et al. Effects of estrogen on global gene expression: identification of novel targets of estrogen action. Cancer Res. 2000; 60:5977–83. [PubMed: 11085516]
7. Chung Y, Jonkers J, Kitson H, et al. A whole-genome mouse BAC microarray with 1-mb resolution for analysis of DNA copy number changes by array comparative genomic hybridization. Genome Res. 2004; 14:188–96. [PubMed: 14707179]
8. Gruvberger S, Ringner M, Chen Y, et al. Estrogen receptor status in breast cancer is associated with remarkably distinct gene expression patterns. Cancer Res. 2001; 61:5979–84. [PubMed: 11507038]
9. Van't Veer LJ, Dai H, van de Vijver MJ, et al. Gene expression profiling predicts clinical outcome of breast cancer. Nature. 2002; 415:530–6. [PubMed: 11823860]
10. Van de Vijver, He YD, van't Veer LJ, et al. A gene-expression signature as a predictor of survival in breast cancer. N Engl J Med. 2002; 347:1999–2009. [PubMed: 12490681]
11. Sotiriou C, Neo S, McShane LM, et al. Breast cancer classification and prognosis based on gene expression profiles from a population-based study. Proc Natl Acad Sci U S A. 2003; 18:10393–8. [PubMed: 12917485]
12. Zhao H, Langerod A, Ji Y, et al. Different gene expression patterns in invasive lobular and ductal carcinomas of the breast. Mol Biol Cell. 2004; 15:2523–36. [PubMed: 15034139]
13. Wang Y, Klijn JGM, Sieuwerts AM, et al. Gene-expression profile to predict distant metastasis of lymph-node-negative primary breast cancer. Lancet. 2005; 365:671–9. [PubMed: 15721472]
14. Rhodes DR, Yu J, Shanker K, et al. ONCOMINE: a cancer microarray database and integrated data-mining platform. Neoplasia. 2004; 6:1–6. [PubMed: 15068665]
15. Elfilali A, Lair S, Verbeke C, La Rosa P, Radvanyi F, Baillot E. ITTACA: a new database for integrated tumor transcriptome array and clinical data analysis. Nucleic Acids Res. 2006; 34:D613–6. [PubMed: 16381943]
16. Cobleigh MA, Vogel CL, Tripathy D, et al. Multinational study of the efficacy and safety oh humanized anti-HER2 monoclonal antibody in women who have HER2-overexpressing metastatic breast cancer that has progressed after chemotherapy for metastatic disease. J Clin Oncol. 1999; 17:2639–48. [PubMed: 10561337]
17. Yin Y, Tainsky MA, Bischoff FZ, Strong LC, Wahl GM. Wild-type p53 restores cell cycle control and inhibits gene amplification in cell with mutant p53 alleles. Cell. 1992; 70:937–48. [PubMed: 1525830]
18. Livingstone LR, White A, Sprouse J, Livanos E, Jacks T, Tlsty TD. Altered cell cycle arrest and gene amplification potential accompany loss of wild-type p53. Cell. 1992; 70:923–35. [PubMed: 1356076]
19. Yasui K, Arii S, Zhao C, et al. TFDP1, CUL4A, and CDC16 identified as targets for amplification at 13q34 in hepatocellular carcinomas. Hepatology. 2002; 35:1476–84. [PubMed: 12029633]
20. Shinomiya T, Mori T, Ariyama Y, et al. Comparative genomic hybridization of squamous cell carcinoma of the esophagus: the possible involvement of the DPI gene in the 13q34 amplicon. Genes Chromosomes Cancer. 1999; 24:337–44. [PubMed: 10092132]
21. Yasui K, Okamoto H, Arii S, Inazawa J. Association of over-expressed TFDP1 with progression of hepatocellular carcinomas. J Hum Genet. 2003; 48:609–13. [PubMed: 14618416]
22. Singhal S, Amin KM, Kruklitis R, et al. Alterations in cell cycle genes in early stage lung adenocarcinoma identified by expression profiling. Cancer Biol Ther. 2003; 2:291–8. [PubMed: 12878869]
23. Chen LC, Manjeshwar S, Lu Y, et al. The human homologue for the *Caenorhabditis elegans* cul-4 gene is amplified and overexpressed in primary breast cancers. Cancer Res. 1998; 58:3677–83. [PubMed: 9721878]

24. Johnson DG, Cress WD, Jakoi L, Nevins JR. Oncogenic capacity of the E2F1 gene. Proc Natl Acad Sci U S A. 1994; 91:12823–7. [PubMed: 7809128]
25. Muller H, Helin K. The E2F transcription factors: key regulators of cell proliferation. Biochim Biophys Acta. 2000; 1470:M1–12. [PubMed: 10656985]
26. Jooss K, Lam EW, Bybee A, Girling R, Muller R, La Thanque NB. Proto-oncogenic properties of the DP family of proteins. Oncogene. 1995; 10:1529–36. [PubMed: 7731707]
27. Sorensen TS, Girling R, Lee C, Gannon J, Bandara LR, La Thangue NB. Functional interaction between DP-1 and p53. Mol Cell Biol. 1996; 16:5888–95. [PubMed: 8816502]
28. Wang D, Russell J, Xu H, Johnson DG. Deregulated expression of DP1 induces epidermal proliferation and enhances skin carcinogenesis. Mol Carcinog. 2001; 31:90–100. [PubMed: 11429786]
29. Nag A, Bagchi S, Raychaudhuri P. Cul4A physically associates with MDM2 and participates in the proteolysis of p53. Cancer Res. 2004; 64:8152–5. [PubMed: 15548678]
30. Gupta A, Yang L, Chen L. Study of the G_2-M cell cycle checkpoint in irradiated mammary epithelial cells overexpressing Cul-4A gene. Int J Radiat Oncol Biol Phys. 2002; 52:822–30. [PubMed: 11849807]
31. Saitoh O, Wang WC, Lotan R, Fukuda M. Differential glycosylation and cell surface expression of lysosomal membrane glycoproteins in sublines of a human colon cancer exhibiting distinct metastatic potentials. J Biol Chem. 1992; 267:5700–11. [PubMed: 1544942]
32. Sawada R, Lowe JB, Fukuda M. E-selectin–dependent adhesion efficiency of colonic carcinoma cells is increased by genetic manipulation of their cell surface lysosomal membrane glycoprotein-1 expression levels. J Biol Chem. 1993; 268:12675–81. [PubMed: 7685349]
33. Sun WS, Fujimoto J, Tamaya T. Coexpression of growth arrest-specific gene 6 and receptor tyrosine kinase Axl and Sky in human uterine endometrial cancers. Ann Oncol. 2003; 14:898–906. [PubMed: 12796028]
34. Stitt TN, Conn G, Gore M, et al. The anticoagulation factor protein S and its relative, Gas6, are ligands for the Tyro3/Axl family of receptor tyrosine kinase. Cell. 1995; 80:661–70. [PubMed: 7867073]
35. Vajkoczy P, Knyazev P, Kunkel A, et al. Dominant-negative inhibition of the Axl receptor tyrosine kinase suppressed brain tumor cell growth and invasion and prolongs survival. Proc Natl Acad Sci U S A. 2005; 103:5799–804. [PubMed: 16585512]
36. Sasaki T, Knyazev PG, Clout NJ, et al. Structural basis for Gas6-Axl signaling. EMBO J. 2006; 25:80–7. [PubMed: 16362042]
37. Holland SJ, Powell MJ, Franci C, et al. Multiple roles for the receptor tyrosine kinase axl in tumor formation. Cancer Res. 2005; 65:9294–303. [PubMed: 16230391]

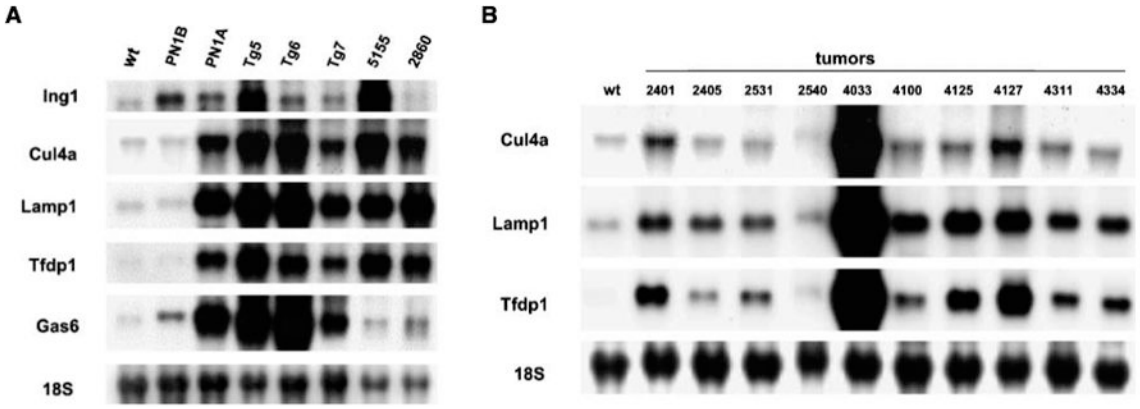

Figure 1.

A, Northern blot analysis of deregulated genes in two p53 null mammary epithelial outgrowth lines: *PN1B*, mildly aggressive low tumorigenic; *PN1A*, highly aggressive and tumorigenic, and five mammary tumors derived from the PN1A outgrowth line (*Tg5*, *Tg6*, *Tg7*, *5155*, and *2860*). *Lane wt*, p53 wild-type normal mammary epithelium. *B*, Northern blot analysis of *Cul4a*, *Lamp1*, and *Tfdp1* in spontaneously generated p53 null mammary tumors (*lanes 2–11*) compared with p53 wild-type normal mammary epithelium (*lane 1*).

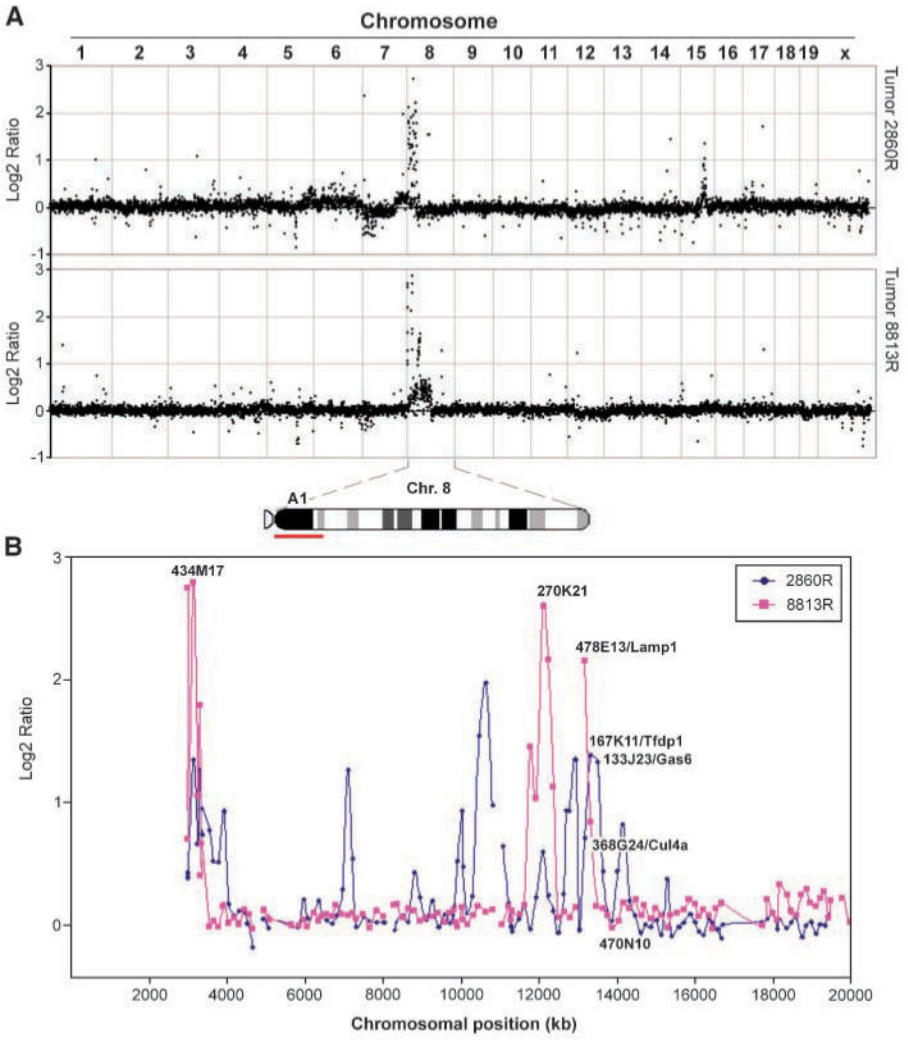

Figure 2.

A, whole-genome mouse BAC microarray CGH of two p53 null mammary tumors. Tumor 2860R (*blue*) was derived from the outgrowth cell line PN1A, and tumor 8813R (*red*) was spontaneously generated. Note the increased in hybridization intensity ratios for the DNA in the area close to the centromere. The amplified region corresponding to band 8A1 is shown on the chromosomal ideogram (*red line*). *B*, detail of the amplified region on the proximal portion of mouse chromosome 8, band A1. *Cul4a*, *Lamp1*, *Tfdp1*, and *Gas6* map to the indicated RP23 BAC clones with high-intensity hybridization ratios, indicative of a gene amplification phenomenon. *X*-axis, relative chromosomal position in kilobases.

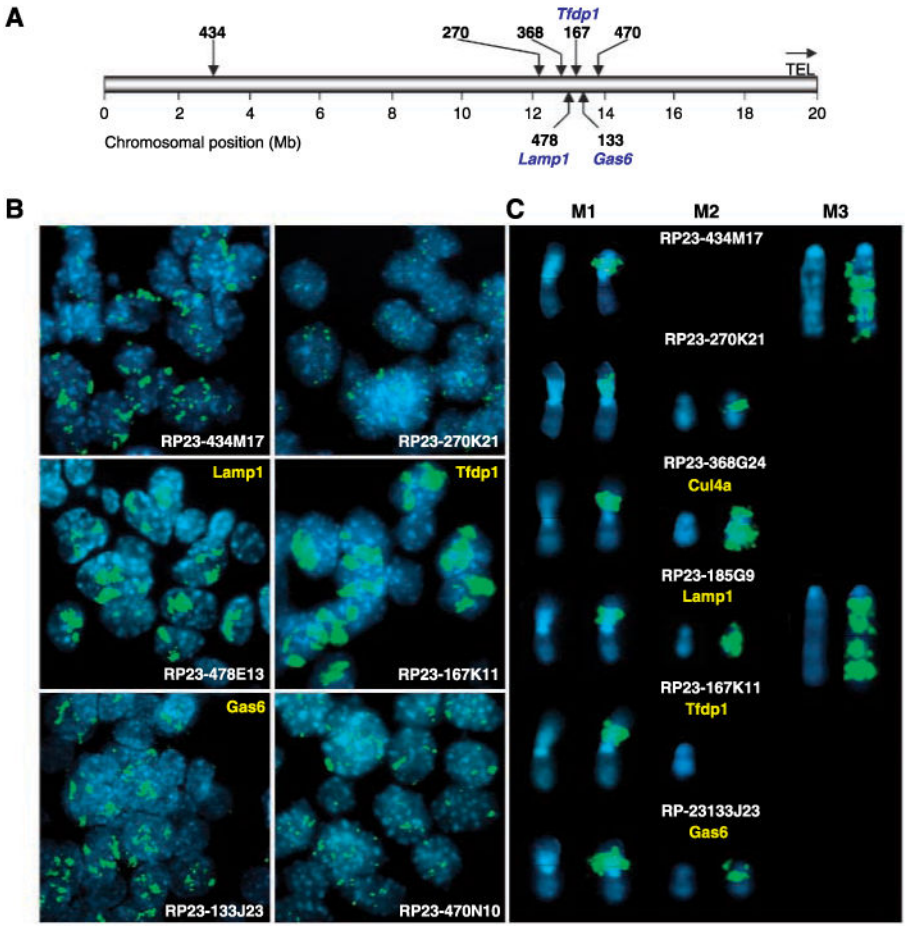

Figure 3.

FISH analyses of p53 null mouse mammary model. *A*, relative position of the BAC clones used as probes in the FISH analyses. *TEL*, telomere. The loci for *Lamp1*, *Tfdp1*, and *Gas6* are indicated. *B*, FISH on touch imprint preparations from a p53 null mouse mammary tumor. Biotin-labeled BAC clones were used as probes. The label was detected with FITC-avidin (*green*), and the nuclei were counterstained with DAPI (*blue*). Note that the genomic regions recognized by RP23 BAC probes 270K21 and 470N10 are not amplified and define the boundaries of the amplicon. *Yellow*, name of genes contained within specific BACs. *C*, cytogenetic and FISH analysis of the PN1A mammary outgrowth line. At least three distinctive chromosomal markers (identified as M1, M2, and M3) displaying homogenously staining regions (*HSR*) were identified on these p53 null mouse mammary premalignant cells. BACs identifying the amplified ch8A1 sequences are shown. *Yellow*, name of genes contained within specific BACs.

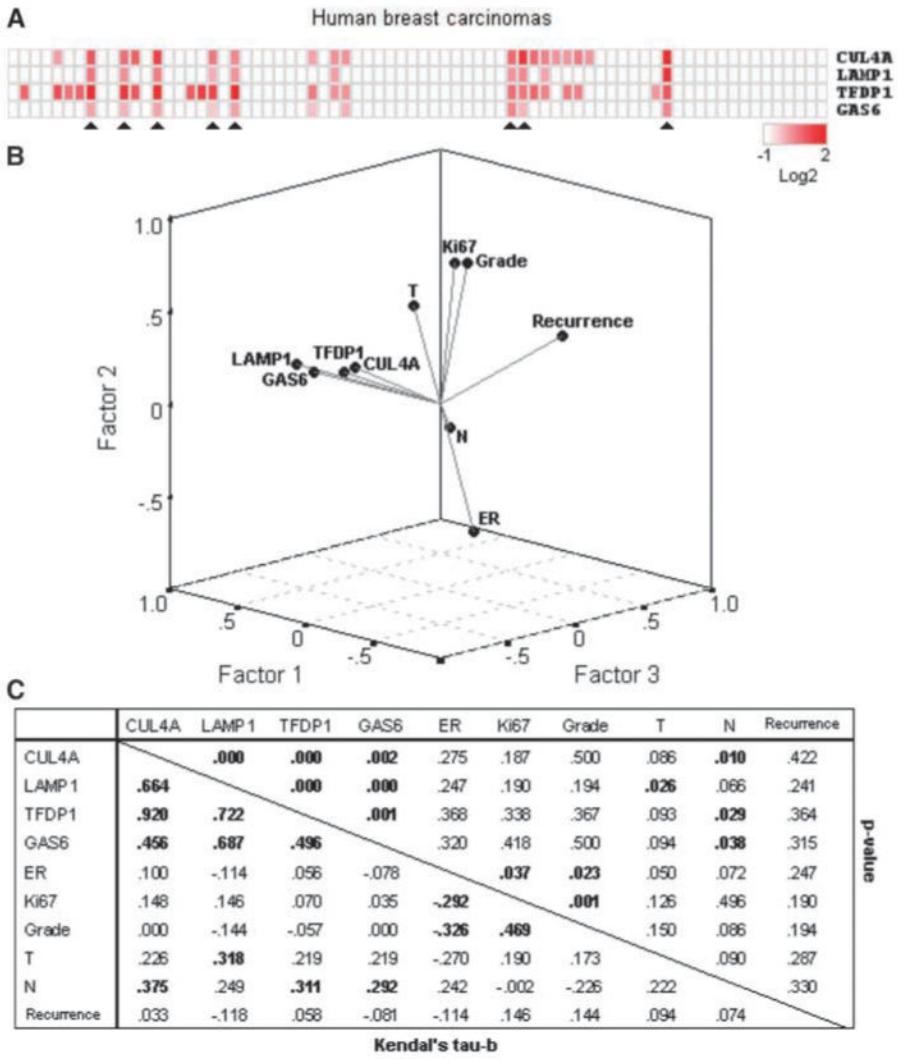

	CUL4A	LAMP1	TFDP1	GAS6	ER	Ki67	Grade	T	N	Recurrence
CUL4A		**.000**	**.000**	**.002**	.275	.187	.500	.086	**.010**	.422
LAMP1	**.664**		**.000**	**.000**	.247	.190	.194	**.026**	.066	.241
TFDP1	**.920**	**.722**		**.001**	.368	.338	.367	.093	**.029**	.364
GAS6	**.456**	**.687**	**.496**		.320	.418	.500	.094	**.038**	.315
ER	.100	-.114	.056	-.078		**.037**	**.023**	.050	.072	.247
Ki67	.148	.146	.070	.035	**-.292**		**.001**	.126	.496	.190
Grade	.000	-.144	-.057	.000	**-.326**	**.469**		.150	.086	.194
T	.226	**.318**	.219	.219	-.270	.190	.173		.090	.287
N	**.375**	.249	**.311**	**.292**	.242	-.002	-.226	.222		.330
Recurrence	.033	-.118	.058	-.081	-.114	.146	.144	.094	.074	

Figure 4.

A, heat map visualization of amplified human breast carcinomas based on quantitative DNA real-time PCR data. Results of 74 primary breast carcinoma analyzed for amplification of *CUL4A*, *LAMP1*, *TFDP1*, and *GAS6* genes. Experiments were done in triplicate for each data point. Results are expressed as log 2 transformation of the mean difference between tumor versus normal control ($P < 0.01$). Red intensity is a representative of mean difference for each breast tumor. Note that these values do not represent specific copy number increases, but are directly proportional to the level of amplification. Note that eight breast carcinomas showed simultaneous amplification for *CUL4A*, *LAMP1*, *TFDP1*, and *GAS6* (*black arrows*). *B*, PCA of 74 breast carcinomas analyzed showing a strong association between the amplification of *CUL4A*, *LAMP1*, *TFDP1*, and *GAS6* genes ($P < 0.001$). *C*, component matrix showing correlation (Kendal's τ -b) and statistical significances (P values) of PCA analysis.

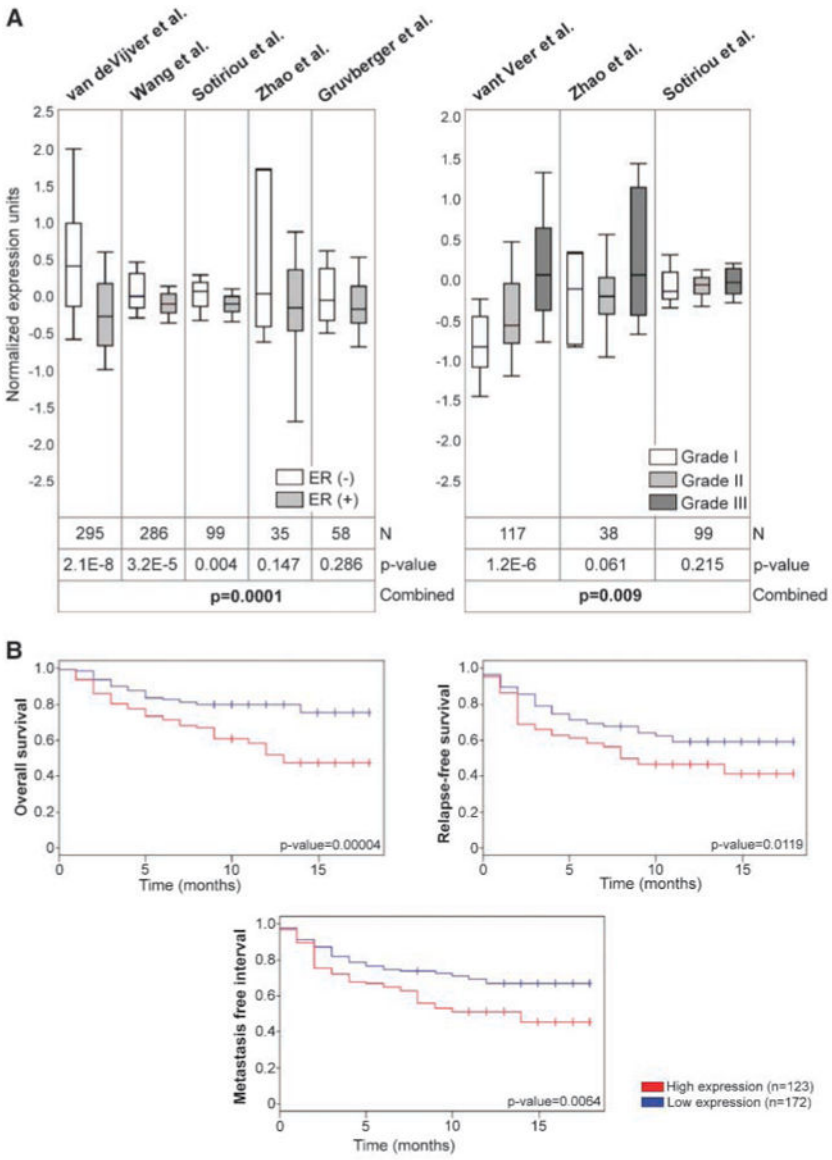

Figure 5.

TFDP1 expression profile of human breast carcinoma using publicly available DNA microarray data sets. *A*, oncomine data output and meta-analysis showing *TFDP1* expression patterns positively associated with ERα(–) breast carcinoma (*left*). Oncomine data output of *TFDP1* expression patterns correlated with high-grade breast carcinoma (*right*). *TFDP1* transcripts are represented in normalized expression units (log 2 data transformed, array media set to 0 and array SD to 1). *B*, Kaplan-Meier curves of overall survival, relapse-free survival, and metastasis-free interval based on high or low expression levels of *TFDP1* gene. Kaplan-Meier analysis was assessed using the Van de Vijver et al. (10) data set by means of ITTACA online resources.

Table 1

Transcripts most significantly up-regulated (fold change, ≥10; $P \leq 0.01$)

SAGE tag	PN1A tumor	p53 null normal	Fold change	Description	Locus
TGGATCCTGA	230	7	33	Hbb-b1 (hemoglobin β major chain)	7 E3
TGCTTAACGA	31	1	31	*RIKEN cDNA 1500015O10 gene*	1 C1
TTAATTGAAC	28	0	28	*Col9a1* (*procollagen type IX α 1*)	1 A5
AGCATCTTCC	**23**	1	**23**	***Tfdp1 (transcription factor Dp 1)***	**8 A1**
GGGGCCTCTG	22	1	22	*Nudtl6* (*nudix*)	16 A1
TGGACCTTTT	20	0	20	*Aldoc* (*aldolase 3, C isoform*)	11 B5
CCCTGAGGGG	369	21	17	*Trf (transferrin)*	9 F1
TTGATCCCCA	**32**	**2**	**16**	***Lamp1 (lysosomal membrane glycoprotein)***	**8 A1**
CTTCTTTCTG	**89**	**6**	**15**	***Gas6*** (***growth arrest specific 6***)	**8 A1**
GGCATTTTAA	**44**	**3**	**15**	***Tfdp1*** (***transcription factor Dp 1***)	**8 A1**
GAAATATATG	99	7	14	*Atp5g3* (*ATP synthase*)	2 C3
ATACACGAAA	**12**	**1**	**12**	***Ing1*** (***inhibitor of growth family 1***)	**8 A1**
GCCACCGTCC	61	6	10	*Nedd4* (*neural precursor cell expression*)	9 D
ATGTTCGTGG	78	8	10	*Dusp6* (*dual specificity phosphat. 6*)	10 C3

NOTE: Detected by SAGE in a p53 null tumor derived from the PN1A mammary outgrowth line (second column) compared with p53 null mammary epithelium (third column). In bold, genes belonging to the same gene linkage group in mouse chr8A1.1.

Cancer Res. Author manuscript; available in PMC 2014 September 17.